THE ASTROPHYSICAL JOURNAL, 600:L167–L170, 2004 January 10

PHOTOMETRIC REDSHIFTS FOR GALAXIES IN THE GOODS SOUTHERN FIELD[1,2]

B. MOBASHER,[3,4] R. IDZI,[5] N. BENÍTEZ,[5] A. CIMATTI,[6] S. CRISTIANI,[7] E. DADDI,[8] T. DAHLEN,[3] M. DICKINSON,[3,5] T. ERBEN,[9] H. C. FERGUSON,[3,5] M. GIAVALISCO,[3] N. A. GROGIN,[5] A. M. KOEKEMOER,[3] M. MIGNOLI,[10] L. A. MOUSTAKAS,[3] M. NONINO,[7] P. ROSATI,[8] M. SCHIRMER,[9,11] D. STERN,[12] E. VANZELLA,[8] C. WOLF,[13] AND G. ZAMORANI[10]

Received 2003 June 5; accepted 2003 July 3; published 2004 January 9

ABSTRACT

We use extensive multiwavelength photometric data from the Great Observatories Origins Deep Survey to estimate photometric redshifts for a sample of 434 galaxies with spectroscopic redshifts in the Chandra Deep Field–South. Using the Bayesian method, which incorporates redshift/magnitude priors, we estimate photometric redshifts for galaxies in the range $18 < R_{AB} < 25.5$, giving an rms scatter $\sigma\,[\Delta z/(1 + z_{spec})] \leq 0.11$. The outlier fraction is less than 10%, with the outlier-clipped rms being 0.047. We examine the accuracy of photometric redshifts for several special subclasses of objects. The results for extremely red objects are more accurate than those for the sample as a whole, with $\sigma = 0.051$ and very few outliers (3%). Photometric redshifts for active galaxies, identified from their X-ray emission, have a dispersion of $\sigma = 0.104$, with 10% outlier fraction, similar to that for normal galaxies. Employing a redshift/magnitude prior in this process seems to be crucial in improving the agreement between photometric and spectroscopic redshifts.

Subject headings: galaxies: fundamental parameters — galaxies: photometry — X-rays: galaxies

1. INTRODUCTION

The successful installation of the Advanced Camera for Surveys (ACS) on board the *Hubble Space Telescope* (*HST*) and the promise of new observatories such as the *Space Infrared Telescope Facility* (*SIRTF*) have opened up new opportunities for multiwavelength surveys of the distant universe. However, most of the galaxies detected in these surveys are too faint for spectroscopic observations. The photometric redshift technique is the only practical way to estimate distances to these galaxies, needed for statistical studies of their properties. The technique has the advantage of providing redshifts for large samples of faint galaxies with a relatively modest investment of observing time but has the disadvantage of having coarse wavelength resolution (~1000 Å) compared to a much higher resolution obtained spectroscopically (~10 Å).

The Great Observatories Origins Deep Survey (GOODS) is designed to reach unprecedented depths in two fields, the Chandra Deep Field–South (CDF-S) and Hubble Deep Field–North (HDF-N), using *HST*, *Chandra*, and *SIRTF*. The majority of the objects detected in GOODS are fainter than the practical limit for spectroscopy. Accurate photometric redshifts are therefore essential in order to estimate distances to galaxies hosting Type Ia supernovae, to convert observable properties (size, color, and magnitude) to those in the rest frame, and to explore many other aspects of galaxy evolution. This Letter provides details of the procedure used to estimate redshifts to galaxies in the GOODS CDF-S and to assess the accuracy with which these are measured, using a sample of galaxies with spectroscopic redshifts. We also test the accuracy of photometric redshifts for special subsamples of objects that have particular scientific interest within the GOODS data set: extremely red objects (EROs) and active galactic nuclei (AGNs).

2. THE SAMPLE

2.1. *Photometric Observations*

We limit our present analysis to the GOODS CDF-S field, where the most complete multiwavelength photometric data are currently available. The imaging data and photometric catalogs are described in Giavalisco et al. (2004). Here, we have used ground-based optical ($U'UBVRI$) and near-infrared (JHK_s) data from ESO facilities (2.2 m Wide Field Imager [WFI], Very Large Telescope [VLT] FORS1, New Technology Telescope Son of ISAAC [SOFI] camera, and VLT Infrared Spectrometer And Array Camera [ISAAC]), as well as from *HST*/ACS ($B_{435}V_{606}i_{775}z_{850}$). Most of the imaging data cover the whole GOODS field of view, but a few (ISAAC JHK_s and FORS1 RI) do not. In total, there are as many as 18 independent pho-

[1] Based on observations taken with the NASA/ESA *Hubble Space Telescope*, which is operated by the Association of Universities for Research in Astronomy (AURA), Inc., under NASA contract NAS5-26555. This work is supported by NASA through grant GO09583.01-96A.

[2] Based on observations collected at the European Southern Observatory, Chile (ESO programmes 168.A-0485, 170.A-0788, 64.O-0643, 66.A-0572, 68.A-0544, 164.O-0561, 169.A-0725, 267.A-5729 66.A-0451, 68.A-0375 164.O-0561, 267.A-5729, 169.A-0725, and 64.O-0621).

[3] Space Telescope Science Institute, 3700 San Martin Drive, Baltimore, MD 21218.

[4] Also affiliated with the Space Sciences Department of the European Space Agency.

[5] Department of Physics and Astronomy, Johns Hopkins University, 3400 North Charles Street, Baltimore, MD 21218-2686.

[6] Instituto Nazionale di Astrofisica, Osservatorio Astrofisico di Arcetri, Largo Enrico Fermi 5, I-50125 Florence, Italy.

[7] Istituto Nazionale di Astrofisica, Osservatorio Astronomico di Trieste, via G.B. Tiepolo 11, Trieste I-34131, Italy.

[8] European Southern Observatory, Karl-Schwarzschild-Strasse 2, D-85748 Garching, Germany.

[9] Institut für Astrophysik und Extraterrestrische Forschung, Universität Bonn, Auf dem Hügel 71, D-53121 Bonn, Germany.

[10] Instituto Nazionale di Astrofisica, Osservatorio Astrofisico di Bologna, via Ranzani 1, I-40127 Bologna, Italy.

[11] Max-Planck-Institut für Astrophysik, Karl-Schwarzschild-Strasse 1, D-85748 Garching bei München, Germany.

[12] Jet Propulsion Laboratory, California Institute of Technology, Mail Stop 169-506, Pasadena, CA 91109.

[13] Department of Physics, University of Oxford, Keble Road, Oxford OX1 3RH, UK.

TABLE 1
COMPARISON BETWEEN PHOTOMETRIC AND SPECTROSCOPIC REDSHIFTS

		FORS2					K20				
		BPZ		χ^2			BPZ		χ^2		
R_{lim}	ODDS	$\sigma(\Delta)$	η	$\sigma(\Delta)$	η	n	$\sigma(\Delta)$	η	$\sigma(\Delta)$	η	n
26.00	All	0.107	0.098	0.220	0.11	163	0.072	0.048	0.140	0.059	270
25.00	All	0.114	0.099	0.110	0.110	141	0.072	0.046	0.142	0.058	261
24.50	All	0.111	0.100	0.113	0.100	111	0.073	0.049	0.146	0.049	246
25.00	=1.00	0.082	0.038	0.083	0.038	78	0.065	0.024	0.068	0.030	165
25.00	>0.99	0.095	0.062	0.098	0.062	113	0.064	0.028	0.067	0.028	246
25.00	>0.95	0.100	0.073	0.102	0.073	124	0.070	0.039	0.073	0.043	255

tometric measurements for each galaxy. We matched the point-spread functions of the images, including the ACS data, as described in Giavalisco et al. (2004). An *R*-band selected catalog was created with SExtractor (Bertin & Arnouts 1996). The photometry used for the photometric redshifts was measured through matched 3″ diameter apertures in all bands.

2.2. *Spectroscopic Observations*

The spectroscopic observations of CDF-S galaxies are from two separate samples:

K20.—A portion of this *K*-selected survey [K_s(Vega) $\leq$ 20; K_s(AB) $\leq$ 21.85; Cimatti et al. 2002a, 2002b] lies within the CDF-S and has reliable spectroscopic redshifts for 271 objects, with a median redshift $\langle z \rangle = 0.85$. Using their spectra, the galaxies were classified as normal (i.e., emission and absorption-line systems) or AGNs.

GOODS/FORS2.—The GOODS team is carrying out an extensive spectroscopic campaign in the CDF-S as an ESO Large Programme (C. Cesarsky, PI). Here, we use data from the first observing season, obtained with the VLT-FORS2 spectrograph using the 300I grism ($R \approx 860$). The primary targets were faint ($z_{850} < 24.5$) red ($i_{775} - z_{850} > 0.6$) galaxies selected from the ACS imaging. A heterogeneous sample of other galaxies was used to fill out the multislit masks. We use 163 redshifts that were measured with good confidence, with a median redshift $\langle z \rangle = 1.05$.

3. PHOTOMETRIC REDSHIFT TECHNIQUE

We matched the spectroscopic and photometric catalogs and used the multicolor data to estimate photometric redshifts for galaxies in the spectroscopic sample. The comparison between photometric and spectroscopic redshifts then gives an estimate of the photometric redshift accuracy. Because the two spectroscopic samples are selected differently, we have analyzed them separately and compare the results to explore any biases induced by color/magnitude selection criteria.

We have performed extensive experiments with two variant methods of photometric redshift estimation: spectral template χ^2 minimization (Puschell, Owen, & Laing 1982) and the Bayesian method of Benítez (2000). In the χ^2 technique, the photometric redshift of a galaxy is estimated by comparing its multiband photometry with spectral energy distribution (SED) templates of galaxies with known types, shifted in redshift space and integrated through the bandpass throughput functions. For each template, at each redshift, the χ^2 statistic is estimated, with the best-fitting redshift and spectral type found from the minimum χ^2 value assigned to the galaxy.

The Bayesian approach considers the distribution $p(z|C, m)$, i.e., the redshift probability given not only the observed colors of a galaxy, *C*, but also its magnitude, *m*. This can be written as (Benítez 2000)

$$p(z|C, m) \propto \Sigma_T p(z, T|m) p(C|z, T).$$

The first term on the right is the redshift/magnitude prior, which contains the probability of a galaxy having redshift *z* and spectral type *T*, given its magnitude *m*, while the second term is the redshift/type likelihood, $p(C|z, T) \propto \exp[-\chi(z, T)^2/2]$.

Note that using a prior of this kind is not equivalent to assuming a particular luminosity function; the prior describes the expected redshift distribution for galaxies of a certain magnitude but does not include information about the galaxy magnitude distribution. The shape of the prior is estimated empirically from the HDF-N observations, as described in Benítez (2000). The best estimate of the redshift, z_B, is then defined as the maximum of $p(z|C, m)$.

We compared results from several different software implementations of the χ^2 method, as well as different choices of the SED templates (empirical or synthetic), and found them to be in generally good agreement with one another and with the Bayesian photometric redshift (BPZ) results up to $z \sim 1$. However, at higher redshifts, the BPZ approach gives significantly better performance, as described in § 4 below. We have used the BPZ software that offers both simple χ^2 minimization as well as the Bayesian estimate. We use template libraries, consisting of E, Sbc, Scd, and Im SEDs from Coleman, Wu, & Weedman (1980) and two starburst SB2 and SB3 templates from Kinney et al. (1996). A two-point interpolation between each pair of templates in the color-redshift space is performed, significantly improving the redshift resolution.

The BPZ uses a quality indicator, the Bayesian ODDS, which can be efficiently used to discard those objects with unreliable photo-*z*'s. The ODDS is defined as the integral of the probability distribution $p(z|C, m)$ within a $0.27(1 + z_B)$ interval centered on z_B. The ODDS would thus be 0.95 for a Gaussian $P(z|C, m)$ with width $\sigma = 0.067(1 + z_B)$, which is the empirically measured accuracy of BPZ in the HDF-N.

4. RESULTS

4.1. *Overall Photometric Redshift Performance*

We quantify the reliability of the photometric redshifts by measuring the fractional error for each galaxy, $\Delta \equiv (z_{phot} - z_{spec}) / (1 + z_{spec})$. We examine the median error, $\langle \Delta \rangle$, the rms scatter, $\sigma(\Delta)$, and the rate of "catastrophic" outliers, η, defined as the fraction of the full sample that has $|\Delta| > 0.2$.

Table 1 presents the comparison between photometric and spectroscopic redshifts for both the K20 and the FORS2 samples, using the complete photometric data set available for each object, and for different combinations of magnitude limits and the

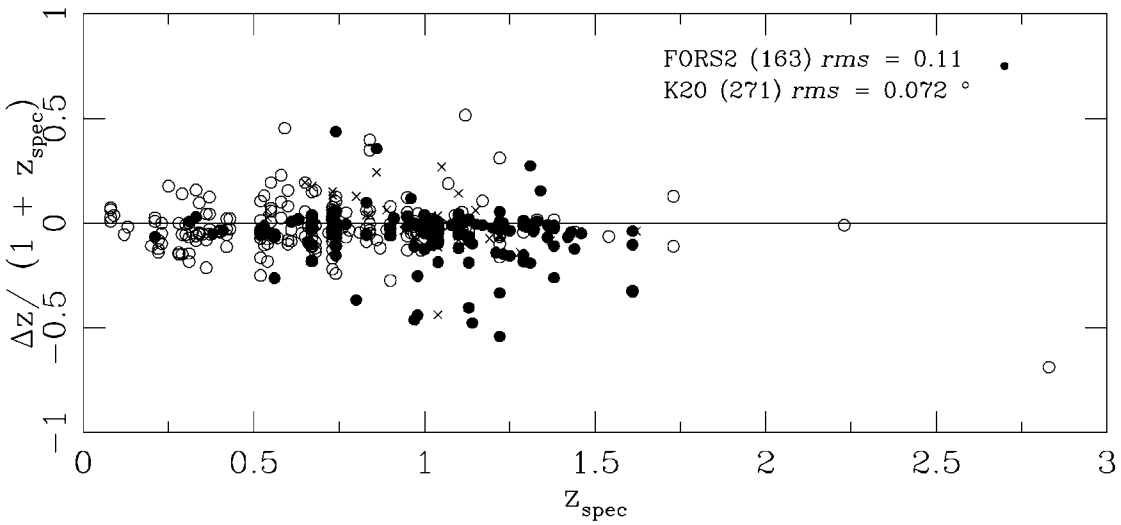

FIG. 1.—Comparison between photometric and spectroscopic redshifts for the K20 (*open circles*) and FORS (*filled circles*) samples. Galaxies undetected (very faint) in U and U' bands in both samples are plotted by crosses.

ODDS parameter. Overall, the BPZ method yields $\sigma(\Delta) \approx 0.11$ and 0.07 for the FORS2 and K20 samples, respectively. At fainter magnitudes ($R_{AB} > 25$), the BPZ method gives smaller rms scatter than the conventional χ^2 minimization technique with no priors. The BPZ results are presented in Figure 1. The agreement between the photometric and spectroscopic redshifts is excellent, with median offset $\langle\Delta\rangle = -0.01$. There is no substantial trend in $\langle\Delta\rangle$ with redshift, except perhaps for a slight tendency for the photometric redshifts to be underestimated at $z > 1.3$. The rms values are all based on a total of 433 galaxies in K20 (270) and FORS2 (163), with the object at $z = 2.8$ excluded (see § 4.2).

For redshifts estimated with Bayesian priors, we find that the fraction of catastrophic outliers, η, ranges from 0.024 to 0.10, depending on the subsample considered. As described in Benítez (2000), the value of the ODDS parameter is a reasonable indicator of the reliability of the photometric redshift; galaxies with larger ODDS values have a smaller probability of being an outlier. We have measured $\sigma(\Delta)$ using only galaxies with $|\Delta| < 0.2$ (i.e., excluding the outliers) and find 0.049 (FORS2) and 0.046 (K20) from the BPZ method. The outlier-clipped rms is similar when using the conventional χ^2 method without priors, but the failure rate, η, from this method is much larger.

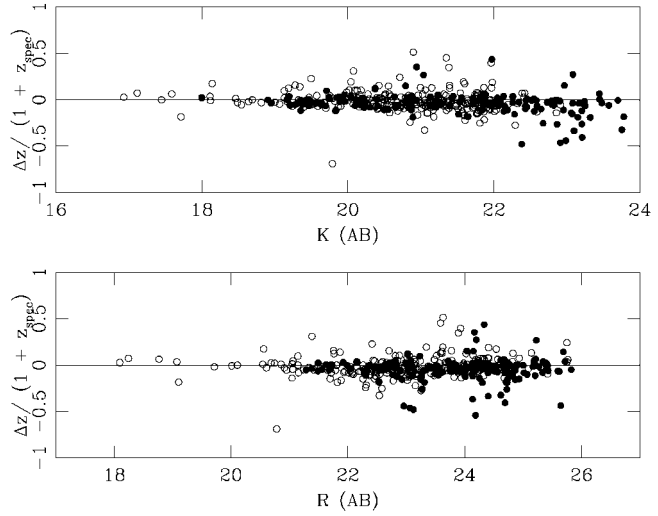

FIG. 2.—Dependence of the accuracy of photometric redshifts to brightness of galaxies in R_{AB} and K_s (AB). Objects from both the K20 (*open circles*) and FORS (*filled circles*) samples are included.

We have estimated redshifts using different combinations of the available photometric data in CDF-S and find no significant differences in the $\sigma(\Delta)$ values. In particular, we have compared the performance with and without using the ACS photometry and found no significant difference in the overall result. The deep ACS photometry, however, may well be important at fainter magnitudes, beyond the limits of the spectroscopic sample. 18% of the FORS2 galaxies and 13% of the K20 galaxies are undetected (less than 3 σ) in the relatively shallow WFI U or U' images. However, we find no significant difference in Δ-values for galaxies with and without U/U' detections down to the spectroscopic magnitude limit (Fig. 1, *crosses*). We have also estimated photometric redshifts using the WFI and SOFI data alone, which cover a wider CDF-S area, including areas not imaged by ACS. We measure $\sigma(\Delta) = 0.11$ (for $R_{AB} < 25$).

Figure 2 plots the redshift errors Δ versus galaxy magnitudes in the R and K_s bands. There is no strong trend in $\sigma(\Delta)$ with magnitude, except at the faintest K_s-band limits, $K_s \gtrsim 22.5$. The outlier fraction η increases from 0.03 ($K_s < 20$) to 0.05 ($20 < K_s < 22$) to 0.11 ($22 < K_s < 24$). The photometric redshifts are also, on average, slightly underestimated for $K_s > 22$. At these faint magnitudes, many of the galaxies are only poorly detected, if at all, in the wide-field (but relatively shallow) SOFI JHK_s images, causing an increase in redshift errors.

Results from Table 1 indicate that the photometric redshift performance is correlated with the ODDS parameter and is better for higher ODDS values (ODDS > 0.99). It is important to remember that the galaxies in the spectroscopic sample are relatively bright compared to the large majority of objects in the GOODS fields. The ODDS parameter, perhaps combined with other indicators (e.g., the number of passbands in which the galaxy is significantly detected, availability of U-band and near-IR data, and the width of the redshift probability distribution), offers a useful metric for the likely reliability of photometric redshifts at magnitudes fainter than the limit of our spectroscopic test sample.

4.2. *Special Galaxy Populations*

One of the main aims of the GOODS project is to identify and study different populations of galaxies, such as EROs and AGNs. In this section we carry out an analysis of the reliability of photometric redshifts to these objects:

EROs.—The GOODS ERO sample is selected to have $(R-K)_{AB} > 3.35$ and is complete to $K_{AB} < 22$ mag. A total of 66 EROs have spectroscopic redshifts in the combined FORS2 (36) and K20 (30) samples. Figure 3*a* compares the photometric and spectroscopic redshifts for EROs. There is an excellent agreement, with $\sigma(\Delta) = 0.051$, and it is equally good for objects classified as absorption- and emission-line systems. Furthermore, we find a very small fraction of outliers ($\eta = 3\%$). This performance is significantly *better* than that for the galaxy sample as a whole. This may not be surprising: in general, red galaxies have stronger features in their broadband SEDs (breaks, curvature) than do blue ones. However, it is a very helpful result because EROs are among the most difficult galaxies for spectroscopic observations.

The ERO population is known to consist of high-redshift ($z \sim 1$) elliptical galaxies and dusty starbursts (Cimatti et al. 2002c). However, the starburst galaxy templates from Kinney et al. (1996) that are used for photometric redshift estimation are not significantly reddened and certainly do not match the colors of EROs. Photometric redshifts for the majority of the EROs, therefore, are derived from the elliptical galaxy spectral template, regardless of the true nature of the galaxies. Moustakas et al. (2004) find that ~40% of the GOODS EROs are morphologically early-type galaxies; the rest are either disk galaxies or irregular systems. However, they also find that the broadband SEDs of the EROs in different morphological subclasses are virtually indistinguishable. Thus, we expect comparably good photometric redshift estimates for most EROs, regardless of their intrinsic nature.

AGNs.—48 galaxies in the spectroscopic K20 (31) and FORS2 (17) samples have X-ray detection (Alexander et al. 2003). Figure 3*b* compares photometric and spectroscopic redshifts for these X-ray sources. The rms scatter, excluding the object at $z = 2.8$, which is confirmed to be a quasi-stellar object, is $\sigma(\Delta) = 0.104$, with an oulier fraction of $\eta = 0.11$. Excluding the five outliers reduces the rms scatter to $\sigma(\Delta) = 0.042$. The majority of the X-ray sources at higher redshifts here are AGNs, although some are likely to be X-ray starbursts. Six of these sources are spectroscopically confirmed as AGNs (Fig. 3*b*, *crosses*). The scatter and the outlier fraction for the X-ray sources (i.e., AGNs) is similar to that for normal galaxies in Figure 1. We tried using an independent set of observed AGN SEDs as templates but did not significantly improve $\sigma(\Delta)$. Using the conventional χ^2 method without priors increases the $\sigma(\Delta)$-value to 0.43.

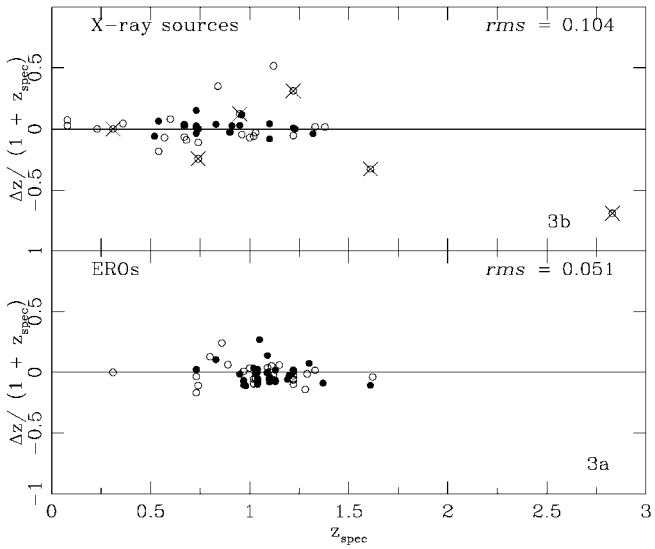

FIG. 3.—(*a*) Comparison between photometric and spectroscopic redshifts. EROs from K20 (*open circles*) and FORS (*filled circles*). (*b*) X-ray sources (i.e., AGNs) from K20 (*open circles*) and FORS2 (*filled circles*), with spectroscopically confirmed AGNs (*crosses*).

5. CONCLUSIONS

Combining multi–wave band ground-based and ACS photometric data (with up to 18 photometric passbands per object), we have estimated photometric redshifts for 433 galaxies with spectroscopic redshifts in the GOODS CDF-S field, using the photometric redshift method of Benítez (2000), which incorporates Bayesian magnitude/redshift priors. We find an overall performance $\sigma(\Delta) = 0.11$, with better performance for some subsamples. The fraction of catastrophic redshift outliers is less than 10% and is substantially smaller for galaxies with high values of the Bayesian ODDS parameter. We see no strong trend in the performance of the photometric redshifts versus magnitudes, except for an increase in the outlier rate. Employing a redshift/magnitude prior in this process seems to be crucial in reducing the scatter between photometric and spectroscopic redshifts.

We have applied the method to two subsamples of galaxies of particular interest: EROs and AGNs. The results for EROs are more accurate [$\sigma(\Delta) = 0.051$] than for normal galaxies in general. They are somewhat less accurate for the X-ray sources (i.e., AGNs)—$\sigma(\Delta) = 0.104$—but good enough to be useful for many applications.

REFERENCES

Alexander, D. M., et al. 2003, AJ, 126, 539
Benítez, N. 2000, ApJ, 536, 571
Bertin, E., & Arnouts, S. 1996, A&AS, 117, 393
Cimatti, A., et al. 2002a, A&A, 392, 395
———. 2002b, A&A, 391, L1
———. 2002c, A&A, 381, L68
Coleman, G. D., Wu, C.-C., & Weedman, D. W. 1980, ApJS, 43, 393
Giavalisco, M., et al. 2004, ApJ, 600, L93
Kinney, A. L., Calzetti, D., Bohlin, R. C., McQuade, K., Storchi-Bergmann, T., & Schmitt, H. R. 1996, ApJ, 467, 38
Moustakas, L. A., et al. 2004, ApJ, 600, L131
Puschell, J. J., Owen, F. N., & Laing, R. A. 1982, ApJ, 257, L57